Journal of Nanoscience and Technology 2(4) (2016) 186–188

ISSN: 2455-0191

Contents List available at JACS Directory

Journal of Nanoscience and Technology

journal homepage: www.jacsdirectory.com/jnst

CTAB Assisted Synthesis of Cobalt Ferrite Nanoparticles and Its Characterizations

A. Persis Amaliya, S. Anand, S. Pauline*

Department of Physics, Loyola College, Chennai – 600 034, Tamil Nadu, India.

ARTICLE DETAILS

Article history:
Received 07 November 2016
Accepted 17 November 2016
Available online 27 December 2016

Keywords:
Magnetic Materials
Sol-Gel Method
CTAB

ABSTRACT

We report here the influence of cetyltrimethylammonium bromide (CTAB) cationic surfactant in the synthesis of cobalt ferrite ($CoFe_2O_4$) nanoparticles via sol-gel method and hence the influence on the structural, morphological and magnetic properties. The formation of single cubic spinel structured pure and CTAB assisted $CoFe_2O_4$ nanoparticles was confirmed using powder X-ray diffraction (PXRD). Fourier transform infrared measurements (FTIR) between 400 and 4000 cm^{-1} confirmed the intrinsic cation vibration modes of spinel structure. Five Raman active modes of pure and CTAB assisted cobalt ferrite were observed from the analysis of Raman spectra. High resolution scanning electron microscopy (HRSEM) analysis exposed the morphology of as synthesized nanoparticles. No significant changes in Saturation magnetization (Ms), coercivity (Hc) and retentivity (Mr) were noted with the addition of CTAB.

1. Introduction

Magnetic nanoparticles have received noteworthy attentions in different fields of engineering and biomedicine as their magnetic performance provides an extensive applications such as magnetic sensors and magnetic drug delivery and so on [1]. The ferrite spinel structure is based on a closed-packed oxygen lattice, in which tetrahedral (A sites) and octahedral (B sites) interstices are engaged by the cations. Spinels with only divalent ions in the tetrahedral sites are called normal spinel, while compounds with the divalent ions in the octahedral sites are called inverse spinel. In the inverse spinel structure, more of the Co^{2+} ions occupy the octahedral site; half of the Fe^{3+} ions also occupy the same site while half of the Fe^{3+} ions stay in tetrahedral site [2].

$CoFe_2O_4$ is one of the important materials belonging to the inverse spinel group with high coercivity and moderate magnetization. Along with these properties, its physical and chemical stability make $CoFe_2O_4$ nanoparticles appropriate for magnetic recording media applications such as audio- video tape and high-density digital recording disks [3, 4]. Due to its fascinating physical properties and technological importance, a number of studies on $CoFe_2O_4$ nanomaterials prepared by different methods, like sol-gel [5], micro-emulsion [6], combustion [7], chemical co-precipitation [8], polymeric precursor [9], hydrothermal [10]etc., have been carried out. However, the sol-gel method provides homogeneous $CoFe_2O_4$ nanoparticles with a controlled decomposition of precursors, and it is a simple and fast way of synthesizing nanoparticles which hints to high quality products at low cost [11].

Addition of trivial amount of dopants (impurities), use of surfactants and reagents, control of pH, reaction time and temperature has drastic effects on the various physical and chemical properties of prepared nanoparticles. Especially the addition of surfactant in the production process of ferrite nanoparticles supports to control the particle growth and agglomeration of the magnetic nanoparticles because of the steric interference and stabilization properties of surfactant. A few researchers have detailed the addition of CTAB surfactant in the synthesis of $CoFe_2O_4$ nanoparticles affect the size and morphology of the particles synthesized over a number of chemical methods [12-20].

In this work, pure and CTAB assisted $CoFe_2O_4$ nanoparticles were synthesized by simple sol-gel method. The effect of the surfactant CTAB on the structural, morphological and magnetic properties of prepared cobalt ferrite nanoparticles was investigated. The synthesized $CoFe_2O_4$ nanocrystallite samples were studied by using X-ray diffraction (XRD), Fourier Transform Infrared (FTIR) and Raman spectroscopy, High Resolution Scanning Electron Microscopy (HRSEM), and Vibrating Sample Magnetometer (VSM).

2. Experimental Methods

2.1 Materials

The raw materials used for sol-gel synthesis of CTAB assisted cobalt ferrite nanoparticles were Ferric nitrate ($Fe(NO_3)_3.9H_2O$), Cobalt nitrate ($Co(NO_3)_2.6H_2O$), CTAB ($C_{19}H_{42}BrN$, 99%) and ethylene glycol ($(C_2H_4(OH)_2$). All the reagents used for the synthesis of CTAB assisted cobalt ferrite nanoparticles were in analytical grade and used as received from Merck Pvt. Ltd, without further purification.

2.2 Synthesis Procedure

Pure cobalt ferrite (S1) nanoparticles were synthesized via sol-gel route using cobalt nitrate, ferric nitrate and ethylene glycol. Metal nitrates were used as metal precursors and oxidizing agents and ethylene glycol as a reducing agent and fuel for the synthesis. Typically cobalt nitrate and ferric nitrate were taken in the mole ratio 1:2. Required quantity of ethylene glycol [$(C_2H_4(OH)_2$] was added and stirred to get clear solution. This solution was transferred to a petri dish and heated around 60 °C -80 °C. The obtained gel was transferred to a silica crucible and heated for 2 hours at 200 °C. The resultant powder was calcined for 3 hours at 600 °C and fine black powder was obtained. CTAB assisted cobalt ferrite nanoparticles (S2) were synthesized by the same procedure given above with added CTAB. CTAB which act as a capping agent reduces the surface tension of the precursor liquid.

2.3 Characterization

The crystalline phases of the prepared sample was characterized by X-Ray Diffraction (XRD) using a SIEMENS D-5000 diffractometer (Cu-Kα radiation with λ = 1.54056 Å) in the range of 2θ=20°-70°. The Fourier transform infrared spectroscopic analyses were recorded by Bruker IFS66V FT-IR spectrometer with scan range of MIR 400-4000 cm^{-1}. The Raman spectroscopic analysis were recorded by using Renishaw's Raman systems in the range of 100-1200 cm^{-1}. The morphology of the prepared sample was studied by high resonance scanning electron microscopy (HRSEM, Quanta 200 FEG). The magnetic properties were measured using Lakeshore VSM 7410 Vibrating Sample magnetometer at the room temperature.

*Corresponding Author
Email Address: paulantovero@yahoo.co.in (S. Pauline)

3. Results and Discussion

3.1 Structural Properties

3.1.1 X-Ray Diffraction (XRD) Analysis

The formation of cobalt ferrite nanoparticles was analyzed by XRD analysis. Fig. 1 shows the XRD plot between Bragg's angle 2θ and the intensity of X-ray for both S1 and S2 samples. The reflection peaks were indexed to the different (hkl) planes corresponding to the single phase cubic spinel belonging to the space group Fd3m. The major characteristic peak (311) and the others peaks (220), (222), (400), (422), (511) and (440) correspond to the inverse ferrites with a cubic symmetry. All the peaks in the pattern well matched with standard JCPDS card No: 22-1086. The formation of single phase cubic spinel structure was evident from the XRD pattern. Lattice parameters for the spinel phase were calculated using the formula,

$$a = (d\sqrt{(h^2+k^2+l^2)})\ \text{Å}$$

where, 'a' is lattice constant, 'd' is inter planar distance; h, k, l are the Miller indices of the crystal planes.

The average crystallite size of S1 and S2 samples were calculated using Scherer's relation,

$$D = \frac{0.9\lambda}{\beta \cos\theta}\ \text{nm}$$

where, D is the average crystallite size, β is the full width at half maximum for the major peak (311), λ is the X-ray wavelength and θ is the Bragg angle. Average Crystallite grain size (D), Lattice parameter (a) of the prepared samples are tabulated in Table 1.

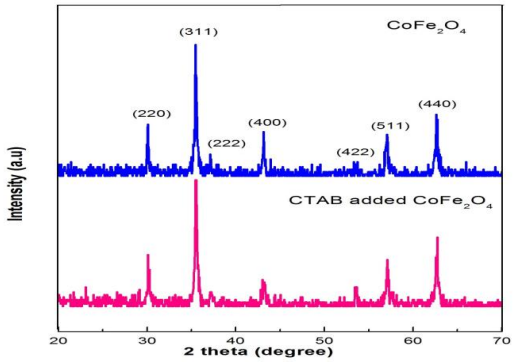

Fig. 1 XRD pattern of pure and CTAB assisted $CoFe_2O_4$ nanoparticles

Table 1 Crystallite size (D), Lattice parameter (a) of the prepared samples

Entry	Sample	Average Crystallite size (D) nm	Lattice parameter(a) Å
1	$CoFe_2O_4$(S1)	34	8.3841
2	$CoFe_2O_4$+CTAB(S2)	29	8.3724

Lattice parameter and average crystallite size were found to be smaller for CTAB added cobalt ferrite. Similar effects on reduction of particle size in the presence of CTAB were reported by Andre-Luis Lopes-Moriyama et al [19].

3.1.2 FTIR and Raman Spectra Analysis

The FT-IR spectra shown in Fig. 2 has all the characteristic bands of $CoFe_2O_4$. Absorption bands attributed to the spinel structure ($v1$ and $v2$) are found to be around 580 cm^{-1} and 410 cm^{-1} respectively. The modes $v1$ and $v2$ are attributed to the cationic vibrations in both octahedral (B) and tetrahedral (A) site of the spinel structure respectively. A band around 1120 cm^{-1} corresponds to Fe-Co alloy; band around 3400 cm^{-1} and 1590 cm^{-1} belongs to O-H stretching vibration, O-H distorted vibration respectively because of adsorbed water by the surface of $CoFe_2O_4$ nanoparticles. Bands at 2916 cm^{-1} and 2352 cm^{-1} are assigned to asymmetric and symmetric stretching of CH_2 groups. The above results well go with the results reported by Anal K. Jha et al and Arokiyaraj, et al [21, 22].

Raman spectra of the as prepared samples are given in Fig. 3. Five Raman active modes of cobalt ferrite $3T_2g$, Eg and A_1g are observed in the spectrum of samples S1 and S2. Eg and T_2g (3) modes correspond to the symmetric and anti-symmetric bending of oxygen atom in (Fe-O and Co-O) bond at octahedral site. A_1g mode is attributed to the motion of oxygen atom around metal ions (Co^{2+}-O, Fe^{3+}-O) in the tetrahedral sites. A_1g sub-band is split from A_1g band (~620 cm^{-1}) and it is caused by partial redistribution of cations [23]. There is no change in the Raman modes of CTAB added sample as compared with pure sample. But a shift towards higher wavenumber is observed at T_2g (1), A_1g (1) modes. This may be due to change in particle size as reported by Chandra Mohan et al [24]. Intensity of peaks reduces with the addition of CTAB. The observed Raman modes for pure (S1) and CTAB assisted $CoFe_2O_4$ nanoparticles (S2) are tabulated in Table 2.

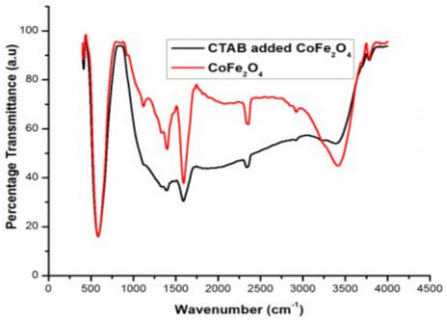

Fig. 2 FTIR pattern of pure and CTAB assisted $CoFe_2O_4$ nanoparticles

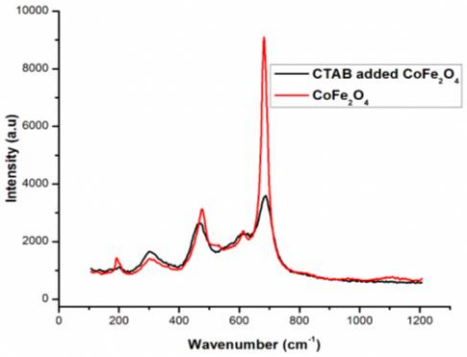

Fig. 3 Raman spectra of pure and CTAB assisted $CoFe_2O_4$ nanoparticles

Table 2 Observed Raman modes for pure (S1) and CTAB assisted $CoFe_2O_4$ nanoparticles (S2)

Entry	Assigned Raman modes	S1	S2
1	$T_2g(3)$	192	201
2	Eg	302	303
3	$T_2g(2)$	475	469
4	$T_2g(1)$	569	575
6	$A_1g(1)$	682	688

3.2 Microstructural Study

The morphology of the as synthesized cobalt ferrite nanoparticles were investigated through High resolution Scanning Electron Microscope (HRSEM). From the Figs. 4(a) and (b) it can be known that the obtained nanoparticles are spherical in shape. The formation of agglomeration in pure $CoFe_2O_4$ nanoparticles is due to the high temperature annealing and interaction between the magnetic particles whereas the reduction of agglomeration in CTAB assisted $CoFe_2O_4$ nanoparticles implies that the adding of CTAB reduces the interactions between the magnetic nanoparticles. Also the nucleation and growth process of cobalt ferrite nanoparticles are significantly controlled by the addition of CTAB and thus affects the size of the nanoparticles.

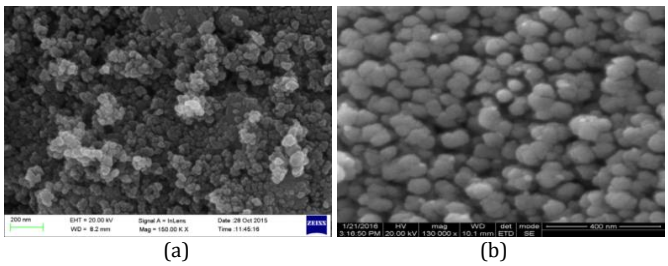

(a) (b)

Fig. 4 HRSEM images of pure (a) and CTAB assisted (b) $CoFe_2O_4$nanoparticles

3.3 Magnetic Properties

3.3.1 Vibrating Sample Magnetometer (VSM) Analysis

Magnetic behavior of pure and CTAB assisted $CoFe_2O_4$ nanoparticles were studied by vibrating sample magnetometer (VSM). Hysteresis loops drawn at room temperature in Fig. 5 indicates the ferromagnetic behavior of the as prepared samples. Measured values from hysteresis loop are listed in Table 3.

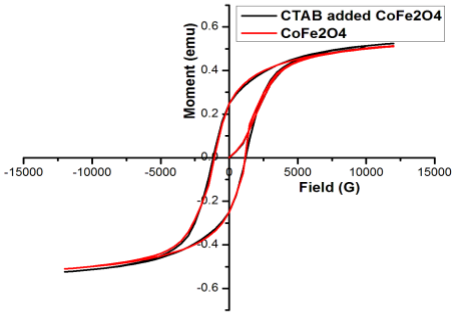

Fig. 5 Hysteresis loops of pure and CTAB assisted $CoFe_2O_4$ nanoparticles

Table 3 Coercivity, Saturation magnetization and Retentivity of as prepared samples

Sample	Coercivity (Hc) Guass	Magnetization (Ms) emu/g	Retentivity (Mr)emu/g
S1	1113	51	24.834
S2	1186	52	24.838

Saturation magnetization (Ms) is the resultant of A and B site magnetization where all the moments are perfectly aligned. Remanent magnetization (Mr) is the magnitude of magnetization present after the saturation and the subsequent removal of the field. Coercivity (Hci) is the magnitude of field required to bring the net magnetization back to zero after field is applied in the direction opposite to the remnant magnetization to randomize magnetic moments [24]. The nearly same value of saturation magnetization for both S1 and S2 sample are in accordance with the small variation in crystallite size from XRD results. The higher value of coercivity is an indication of higher anistrotropic distribution of domains.

4. Conclusion

Pure $CoFe_2O_4$ nanoparticles and $CoFe_2O_4$ nanoparticles with surfactant CTAB were successfully prepared by sol-gel method with high yield. Powder X-Ray Diffraction (PXRD) analysis confirmed the prepared samples as single phase cubic spinel structure. Crystallite grain size and lattice parameter are decreased very feebly when CTAB was used in the synthesis of $CoFe_2O_4$ when compared that of pure $CoFe_2O_4$. The FTIR spectrum images show two absorptions bands in the range of 700-400 cm^{-1} revealing vibrational bands on the formation of spinel cobalt ferrite. The vibrational bands show strong influence of CTAB assisting on cobalt ferrite. Raman spectra well matched with previous studies and particle size reduction caused shift towards higher wavenumber and intensities of peaks reduced for CTAB added cobalt ferrite. Thus the present work concludes that a still higher percentage of CTAB surfactant may affect drastically the structural, morphological and magnetic properties.

Acknowledgement

The authors are thankful to SAIF, IIT Madras, Chennai, for providing HRSEM, FTIR and VSM analysis.

References

[1] M. Arruebo, R. Fernandez-Pacheco, M.R. Ibarra, J. Santamaria, Magnetic nanoparticles for drug delivery, Nano Today 2(3) (2007) 22-32.
[2] A. Goldman, Modern ferrite technology, 2nd Ed., Springer, Pittsburgh, USA, 2006.
[3] V. Pillai, D.O.J. Shah, Synthesis of high-coercivity cobalt ferrite particles using water- in -oil micro emulsions, Magn. Magn. Mater. 163 (1996) 243-248.
[4] R. Skomski, Nano magnetics Topical Review, J. Phys. Condens. Matter 15 (2003) R841-R896.
[5] B.G. Toksha, S.E. Shirsath, S.M. Patange, K.M. Jadhav, Structural investigations and magnetic properties of cobalt ferrite nanoparticles prepared by sol gel auto combustion method, Solid State Commun. 147(11) (2008) 479-483.
[6] J. Fu, J. Zhang, Y. Peng, J. Zhao, G. Tan, et al, Unique magnetic properties and magnetization reversal process of $CoFe_2O_4$ nanotubes fabricated by electro spinning, Nanoscale 4(13) (2012) 3932-3936.
[7] N.M. Deraz, Glycine-assisted fabrication of monocrystalline cobalt ferrite system, J. Anal. Appl. Pyrolysis 88(2) (2010) 103-109.
[8] M.P. Gonzalez-Sandoval, A.M. Beesley, M. Miki-Yoshida, L. Fuentes-Cobas, J.A. Matutes-Aquino, Comparative study of the microstructural and magnetic properties of spinel ferrites obtained by co-precipitation, J. Alloys Compd. 369(1) (2004) 190-194.
[9] R.A. Candeia, M.I.B. Bernardi, E. Longo, I.M.G. Santos, A.G. Souza, Synthesis and characterization of spinel pigment $CaFe_2O_4$ obtained by the polymeric precursor method, Mater. Lett. 58(5) (2004) 569-572.
[10] Z. Wang, X. Liu, M. Lv, P. Chai, Y. Liu, et al, Preparation of one-dimensional $CoFe_2O_4$ nanostructures and their magnetic properties, J. Phys. Chem. C 112(39) (2008) 15171-15175.
[11] A. Ghasemi, S. Ekhlasi, M. Mousavinia, Effect of Cr and Al substitution cations on the structural and magnetic properties of $Ni_{0.6}Zn_{0.4}Fe_{2-x}Cr_{x/2}Alx_{/2}O_4$ nanoparticles synthesized using the sol-gel auto-combustion method, J. Mag. Mag. Mat. 354 (2014) 136-145.
[12] H.F. Lu, R.Y. Hong, H.Z. Li, Influence of surfactants on co-precipitation synthesis of strontium ferrite, J. Alloy. Compd. 509 (2011) 10127-10131.
[13] Y. Du, H. Gao, X. Liu, J. Wang, P. Xu, et al, Solvent-free synthesis of hexagonal barium ferrite ($BaFe_{12}O_{19}$) particles, J. Mater. Sci. 45 (2010) 2442-2449.
[14] U. Kurtan, R. Topkaya, A. Baykal, M.S. Toprak, Temperature dependent magnetic properties of $CoFe_2O_4$/CTAB nanocomposites synthesized by sol-gel auto-combustion technique, Ceram. Int. 39 (2013) 6551-6558.
[15] G.B. Ji, S.L. Tang, S.K. Ren, F.M. Zhang, B.X. Gu, et al, Simplified synthesis of single-crystalline magnetic $CoFe_2O_4$ nanorods by a surfactant-assisted hydrothermal process, J. Cryst. Growth 270 (2004) 156-161.
[16] K. Gandha, K. Elkins, N. Poudyal, J.P. Liu, Synthesis and characterization of $CoFe_2O_4$ nanoparticles with high coercivity, J. Appl. Phys. 117(17) (2015) 17A736.
[17] L. Zhao, H. Zhang, Y. Xing, S. Song, S. Yu, et al, Studies on the magnetism of cobalt ferrite nanocrystals synthesized by hydrothermal method, J. Solid State Chem. 181 (2008) 245-252.
[18] J.L. Cao, Z.L. Yan, Y. Wang, G. Sun, X.D. Wang, et al, CTAB-assisted synthesis of mesoporous $CoFe_2O_4$ with high carbon monoxide oxidation activity, Mater. Lett. 106 (2013) 322-325.
[19] A.L.L. Moriyama, V. Madigou, C.P. Souza, C. Leroux, Controlled synthesis of $CoFe_2O_4$ nano-octahedra, Powder Technol. 256 (2014) 482-489.
[20] M. Vadivel, R. RameshBabu, K. Ramamurthi, M. Arivanandhan, CTAB cationic surfactant assisted synthesis of $CoFe_2O_4$ magnetic nanoparticles, Ceram. Inter. 42 (2016) 19320–19328.
[21] A.K. Jha, Kamal Prasad, Biological synthesis of cobalt ferrite nanoparticles, 2nd Ed., Nanotechnology Development, PAGE Press, Italy, 2012, pp.46-51.
[22] S. Arokiyaraj, M. Saravanan, N.K. UdayaPrakash, M. ValanArasu, B. Vijayakumar, et al, Enhanced antibacterial activity of iron oxide magnetic nanoparticles treated with *Argemone mexicana* L. leaf extract: an in vitro study, Mat. Res. Bulletin 48 (2013) 3323-3327.
[23] P. Chandramohan, M.P. Srinivasan, S. Velmurugan, S.V. Narasimhan, Cation distribution and particle size effect on Raman spectrum of $CoFe_2O_4$, J. Solid State Chem. 184 (2011) 89-96.
[24] N.A. Frey, Sheng Peng, Kai Cheng, Shouheng Sun, Magnetic nanoparticles: synthesis, functionalization, and applications in bio imaging and magnetic energy storage, Chem. Soc. Rev. 38 (2009) 2532-2542.